Free Radical Biology & Medicine 52 (2012) 142–150

Contents lists available at SciVerse ScienceDirect

Free Radical Biology & Medicine

journal homepage: www.elsevier.com/locate/freeradbiomed

Original Contribution

Reactive oxygen species are produced at low glucose and contribute to the activation of AMPK in insulin-secreting cells

Alexandre Sarre [a,*], Jessica Gabrielli [a], Guillaume Vial [b], Xavier M. Leverve [b,1], Françoise Assimacopoulos-Jeannet [a]

[a] Department of Cell Physiology and Metabolism, Medical Faculty, University of Geneva, CH 1211 Geneva 4, Switzerland
[b] Laboratoire de Bioénergétique Fondamentale et Appliquée, INSERM U884, Université Joseph Fourier, 38041 Grenoble, France

ARTICLE INFO

Article history:
Received 20 June 2011
Revised 5 October 2011
Accepted 10 October 2011
Available online 18 October 2011

Keywords:
Superoxide
Mitochondria
Complex I
Aconitase
INS1E cells
AMPK
ACC
Free radicals

ABSTRACT

Excess reactive oxygen species (ROS) production is thought to play a key role in the loss of pancreatic β-cell number and/or function, in response to high glucose and/or fatty acids. However, contradictory findings have been reported showing that in pancreatic β cells or insulin-secreting cell lines, ROS are produced under conditions of either high or low glucose. Superoxide production was measured in attached INS1E cells as a function of glucose concentration, by following in real time the oxidation of dihydroethidine. Minimal values of superoxide production were measured at glucose concentrations of 5–20 mM, whereas superoxide generation was maximal at 0–1 mM glucose. Superoxide generation started rapidly (15–30 min) after exposure to low glucose and was suppressed by its addition within minutes. Superoxide was totally suppressed by rotenone, but not myxothiazol, suggesting a role for complex I in this process. Indirect evidence for mitochondrial ROS generation was also provided by a decrease in aconitase activity. Activation of AMPK, a cellular metabolic sensor, and its downstream target ACC by low glucose concentration was largely inhibited by addition of MnTBAP, a MnSOD and catalase mimetic that also totally suppressed superoxide production. Taken together, the data show that low glucose activates AMPK in a superoxide-dependent, AMP-independent way.

Excessive reactive oxygen species (ROS) produced by the mitochondria are considered to play a central role in cellular dysfunction as observed in several pathophysiological states, including obesity, diabetes and its complications, ischemic reperfusion injury, degenerative diseases, and aging [1,2].

In diabetes, these dual effects of ROS are well illustrated by their long-term deleterious effects on insulin-secreting and insulin target cells, as well as on endothelial cells [4], and by the recent demonstration of their contribution to the beneficial effects of exercise on insulin resistance [5].

In pancreatic β cells, a key role has been attributed to ROS produced by excess glucose and/or lipids (glucolipotoxicity) or by proinflammatory cytokines, in the loss of β-cell mass and/or function [6,7], in particular because these cells express low levels of ROS-scavenging enzymes [8–10]. Evidence that this cellular damage is the consequence of a sustained increase in ROS comes from the observation that it is prevented by the normalization of mitochondrial ROS production after the addition of inhibitors of mitochondrial metabolism or by the overexpression of uncoupling protein-1 or manganese superoxide dismutase (MnSOD) [11].

However, the exact relationship between glucose level and reactive oxygen species generation in pancreatic β cells is still debated. Although a positive correlation between glucose level and ROS production has been demonstrated in rat islets [12], and other studies provided evidence that these ROS are a metabolic signal participating in glucose-stimulated insulin secretion [13,14]. By contrast, studies measuring either superoxide or hydrogen peroxide generation in isolated rat β cells show that the production of these two compounds is increased at low glucose, in particular in β cells with higher metabolic responsiveness to glucose [15]. A similar increase in ROS production at low glucose concentration has been reported in several insulin-secreting cell lines [16,17].

AMP-activated protein kinase (AMPK) is a metabolic sensor activated by an increase in the AMP/ATP ratio, i.e., during metabolic stress, exercise, or hypoxia. This activation turns off anabolic pathways consuming ATP and turns on catabolic pathways producing ATP, such as fatty acid oxidation. In addition to the classical pathway of activation by AMP, recent studies have identified in various cell types other physiological activators of this kinase, among which are ROS [18].

* Corresponding author at: Cardiovascular Assessment Facility, CHUV, CH 1005 Lausanne, Switzerland.
E-mail address: alexandre.sarre@chuv.ch (A. Sarre).
[1] Deceased.

0891-5849 © 2011 Elsevier Inc. Open access under CC BY-NC-ND license.
doi:10.1016/j.freeradbiomed.2011.10.437

In this study the relationship between glucose level and superoxide production was determined in real time in INS1E cells. The results show that superoxide production is rapidly increased when the cells are exposed to low glucose concentration, is reversible, and takes place at respiratory complex I. They also suggest that the ROS produced at low glucose play a role in the activation of AMP-activated protein kinase, independent of AMP level.

Materials and methods

Reagents and antibodies

All chemical were from Sigma Chemical (St. Louis, MO, USA). Diphenyleneiodonium chloride (DPI), apocynin, rotenone, N^G-nitro-L-arginine methyl ester, myxothiazol, *N*-acetyl-L-cysteine (NAC), Tempol (4-hydroxy-2,2,6,6-tetramethylpiperidine-1-oxyl), and STO-609-acetic acid were from Sigma. MnTBAP (Mn(III) tetrakis(4-benzoic acid) porphyrin chloride) was from Calbiochem.

Antibodies against phospho-AMPK (Thr172), phospho-liver kinase B1 (LKB1) (Ser428), and phospho-p70S6K (Thr389) were from Cell Signaling. Antibody against phospho-acetyl-CoA carboxylase (ACC) (Ser79) was from Upstate, antibody against phospho-LKB1 (Ser307) was from Biosource and antibody against GAPDH was from Chemicon International. Secondary antibodies were from Bio-Rad Laboratories GmbH (München, Germany).

Cell culture and experimental design

The INS1E cells were cultured in RPMI 1640 medium containing 11 mM glucose supplemented with 5% heat-inactivated fetal calf serum (FCS), 10 mM Hepes, 1 mM pyruvate, 50 μM β-mercaptoethanol, 100 U/ml penicillin, and 100 μg/ml streptomycin as previously described [19,20].

Experiments were performed in multiwell plates (6 or 24 wells) after 3–4 days of culture. All the experiments were performed in RPMI medium containing 1% FCS, 10 mM Hepes, and the indicated glucose concentration.

Measurement of oxidant stress

ROS generation was assessed using the nonfluorescent probe dihydroethidine (DHE). This compound becomes fluorescent when it reacts with superoxide and is considered a specific marker of this reactive oxygen species [21].

Cells in 24-well plates were washed in KRBH 0.07% bovine serum albumin (BSA) and preincubated in RPMI medium at various concentrations of glucose for the times indicated. The cells were then loaded with 5 μM DHE in the medium for 30 min and transferred to a thermostated plate reader (Fluostar Optima; BMG Labtechnologies, Offenburg, Germany).

The fluorescence, expressed in arbitrary units (a.u.), was measured for 30 min every 30 s using an excitation wavelength of 544 nm and an emission wavelength of 590 nm. The slope of the fluorescent signal versus time represented the rate of superoxide production and was expressed as a.u. per second.

Measurement of aconitase activity

Mitochondrial aconitase activity was measured by following the appearance of NADPH at 340 mM [22]. The cells were incubated in six-well plates at the indicated conditions and washed in cold phosphate-buffered saline (PBS). The proteins were extracted in 50 mM Tris–HCl, pH 7.4, buffer containing 0.6 mM $MnCl_2$ and 2 mM Na citrate. After scraping, sonication, and centrifugation for 3 min at 10,000 rpm at 4 °C, 100 μg protein was added to 1 ml reaction solution (50 mM Tris, pH 7.4, 0.6 mM $MnCl_2$, 0.2 mM $NADP^+$, 5 mM Na citrate, and 1 U/ml isocitrate dehydrogenase). The appearance of NADPH was monitored every 3 min at 340 nm for 1 h. Aconitase activity was calculated from the linear increase in absorbance during the last half of the 60-min assay. Activity was calculated by using the extinction coefficient for NADPH of $6.22 \times 10^3\ M^{-1}\ cm^{-1}$ and assuming the conversion of one molecule of citrate to one molecule of NADPH via citrate dehydrogenase [22].

Measurement of reduced glutathione (GSH) content

The cells were treated as for aconitase measurement. At the end of experiment, they were washed with cold PBS and GSH and protein was extracted by adding cold 5% 5-sulfosalicylic acid dihydrate and vigorously vortexing. Cell extract was incubated at 4 °C for 10 min followed by centrifugation for 10 min at 14,000 rpm and 4 °C. The supernatant was diluted 1:5 with Assay Buffer from Arbor Assays.

GSH and total glutathione were measured using the DetectX glutathione fluorescent detection kit and protocol from Arbor Assays. The kit utilizes a nonfluorescent molecule, ThioStar, which covalently binds to the free thiol group on GSH to yield a highly fluorescent product. The fluorescent product is read at 510 nm in a fluorescence plate reader with excitation at 390 nm.

Measurement of nucleotides

The cells were treated as for aconitase measurement and nucleotides were extracted by adding 0.6 ml of 0.6 M $HClO_4$ to the cells and scraping. The extract was centrifuged and an aliquot of the supernatant neutralized with 2.7 M K_2CO_3.

Samples were acidified at pH 3 and separated at 30 °C on a C18 column (Chromsep Microspher C18 Varian France). Nucleotides were eluted in 25 mM sodium pyrophosphate (pH 5.75) at a flow rate of 1 ml/min. Absorbance was measured at 254 nm by a spectrometer integrated into the HPLC (L4200 UV Detector; Merck USA). Areas of peaks were quantified and converted to molar quantities by comparison with AMP, ADP, and ATP standards.

Immunostaining

INS1E cells were seeded on poly-L-ornithine-coated glass coverslip in cell culture medium and cultured 3 days. At the end of the protocol, the cells were washed two times in cold PBS and fixed in 4% paraformaldehyde for 20 min at room temperature (RT). After permeabilization in PBS, 0.5% BSA, and 0.2% Triton X-100 for 15 min at RT, the cells were blocked in PBS, 0.5% BSA, and 0.05% Triton X-100 for 30 min at RT. The cells were then incubated overnight in the same buffer containing anti-LKB1 (Ley 37D/G6) antibody (Santa Cruz Biotechnology) at 1/1000 dilution. After being washed, the cells were incubated with a fluorescein-coupled IgG antibody (Invitrogen). Nuclei were then stained by incubation with 5 μg/ml DAPI for 3 min. Cells were visualized by fluorescence microscopy (Axioskop 2 equipped with an Axiocam color CCD camera). Images were recorded and treated through the Axiovision software (Zeiss, Germany).

Western blotting

At the end of the experiment, the cells were lysed in a lysis buffer containing 250 mM NaCl, 50 mM Hepes, 0.1% Nonidet P-40, 1 mM Na_3VO_4, 2.5 mM NaF, 0.5 mM phenylmethylsulfonyl fluoride, and protease and phosphatase inhibitors (Sigma Chemical). Proteins were measured using the Bio-Rad protein assay (Bio-Rad Laboratories GmbH), with BSA as standard.

Thirty micrograms of proteins was subjected to electrophoresis on a polyacrylamide gel (6 or 12% depending of the molecular weight of the protein of interest), electrotransferred to Immobilon P membranes (Millipore Corp., Bedford, MA, USA), blocked with 2.5% Top

Block (VWR International AG, Luzern, Switzerland) or 5% nonfat milk in phosphate-buffered saline, 0.1% Tween, and incubated overnight at 4 °C in the same buffer containing the antibody. After being washed, the membranes were incubated with a horseradish peroxidase (HRP)-coupled IgG antibody for 1 h at room temperature. The resolved bands were visualized by UptiLight HRP blot chemiluminescent substrate (Uptima, Interchim, Montluçon, France) and exposed to Hyperfilm ECL (Amersham, Buckinghamshire, UK) for 1 to 10 min. The signal was semiquantitatively analyzed using scanning densitometry (Quantity One software; Bio-Rad). Protein bands were normalized to the expression of GAPDH in the same sample.

Statistical analysis

Results are presented as means ± SEM of the indicated number of independent experiments. Statistical analysis was performed using ANOVA with Tukey's post hoc correction or Student's *t* test using SPSS software. When nonparametric tests were required, statistical analysis was performed using the Kruskal–Wallis test with Dunn's post hoc analysis or Mann–Whitney. Differences were considered significant when $p<0.05$.

Results

Superoxide production is rapidly and reversibly increased by low glucose and inhibited by rotenone

The rate of superoxide production was determined in real time by following the oxidation of DHE. DHE is an intracellular fluorescent probe known to be specific for superoxide [21]. Initially, the experiments were performed in KRB medium containing 10 mM Hepes and 1% BSA and similar results were obtained. To minimize a possible

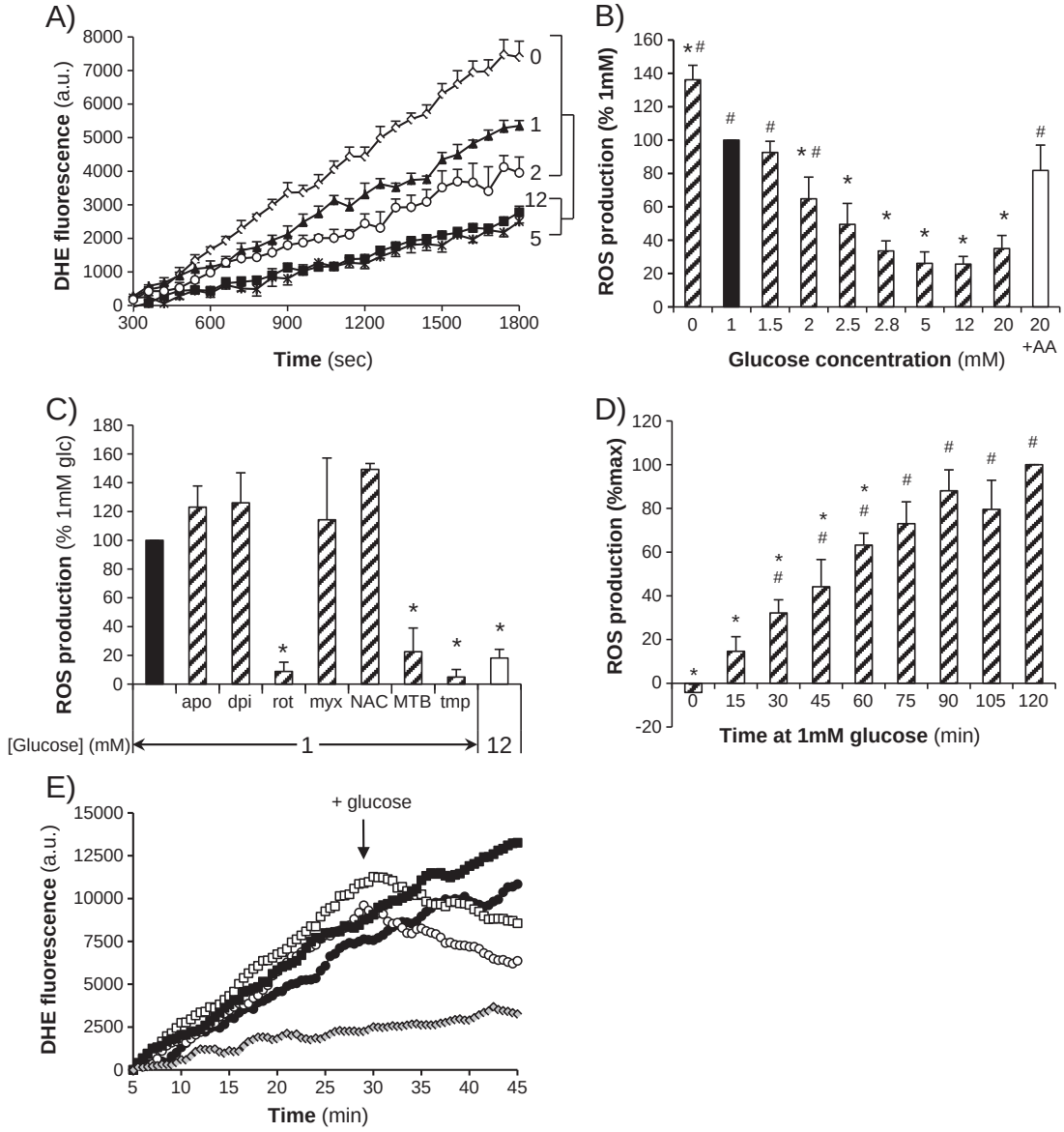

Fig. 1. Pattern of ROS production at low glucose. (A) Representative experiment of real-time ROS measurement by dihydroethidine (5 μM) after 60 min incubation at increasing glucose concentrations. Number at the end of each curve indicates glucose concentration (mM). For the sake of clarity, only one point every 60 s is reported ($n=4$). (B) Quantification of the slopes of ROS production at increasing glucose concentration, expressed in % of 1 mM glucose. Measurements were performed after 60 min incubation at the indicated glucose concentration ($n=4$–11). (C) ROS production at low glucose was totally inhibited by complex I inhibitor and by superoxide scavengers: apo, apocynin; dpi, diphenyleneiodonium; rot, rotenone; myx, myxothiazol; NAC, *N*-acetylcysteine; MTB, MnTBAP; tmp, Tempol ($n=3$–12). (D) Time course of ROS production at 1 mM glucose, expressed in % of that measured at 120 min ($n=3$–9). (E) Representative experiment showing that ROS production at 1 mM glucose was reversed when 11 mM glucose was added (arrow, open symbol curves). Black symbols, 1 mM glucose; gray diamond, measurement at 12 mM glucose. Means ± SEM; $^*p<0.05$ vs 1 mM glucose; #$p<0.05$ vs 12 mM glucose.

contribution of stress due to the lack of amino acids, all the experiments presented were performed in RPMI medium containing 1% FCS. Cells were exposed to 0, 1, 2, 5, 12, and 20 mM glucose for the indicated times and then superoxide production was measured for 30 min. Fig. 1A shows the time course of DHE fluorescence intensity measured in INS1E cells. Compared to 12 mM glucose, a significant increase in the slope of this fluorescence, representing the rate of superoxide production, was observed at glucose concentrations of 2 mM and lower ($p<0.01$). The glucose dose dependence of superoxide production shows minimal values at 5 and 12 mM and a gradual increase at lower concentration. One hour of exposure to high glucose concentration (20 mM) did not significantly increase superoxide production, nor did exposure to high glucose for up to 24 h (data not shown). Addition of antimycin A, an inhibitor of complex III of the mitochondrial respiratory chain, known to induce superoxide production, was also used to validate the measurement (Fig. 1B).

To determine the source of this superoxide production, inhibitors of the main intracellular sources of ROS were used. The nonspecific flavoenzyme inhibitor DPI and the specific NADPH oxidase inhibitor apocynin, both used as inhibitors of NADPH oxidases, and the specific mitochondrial respiratory chain complex III inhibitor myxothiazol had no effect on superoxide production measured after 1 h incubation at 1 mM glucose (Fig. 1C). However, rotenone, a specific inhibitor of complex I of the respiratory chain, completely abolished superoxide production at low glucose. The two ROS-scavenging enzyme mimetics used, MnTBAP (a MnSOD and catalase mimetic [23]) and Tempol (a MnSOD mimetic), abolished the DHE fluorescent signal, whereas NAC, which is a hydrogen peroxide scavenger, had no effect on DHE signal. These results show that superoxide produced at 1 mM glucose was mainly formed at the level of mitochondrial complex I. The time course at low glucose (Fig. 1D) shows that an increase in the rate of superoxide production was measured after 15 min exposure to 1 mM glucose and became significant after 30 min. This rate increased progressively up to 60 min and then remained constant. In addition, when 11 mM glucose was added (i.e., a final concentration of 12 mM), the slope of the fluorescence signal rapidly decreased (Fig. 1E), indicating that this superoxide production is reversible.

Superoxide production is accompanied by a decreased aconitase activity

Indirect evidence of mitochondrial ROS generation was provided by the measurement of aconitase activity, considered as a sensor of mitochondrial oxidative stress. This critical citric acid cycle enzyme is a member of the family of [4Fe–4S]-containing dehydratases that is inactivated by oxidation of the iron atom of the $[4Fe–4S]^{2+}$ center [22]. In our experiments, aconitase activity was decreased by about 25% after 60 min at 1 mM glucose. This decrease was comparable to that measured after 10 min exposure to 25 μM H_2O_2, whereas 50 μM induced a much larger decrease (Fig. 2A).

Free GSH content remained unchanged for 60 min and tended to decrease after 90 min of culture at 1 mM glucose (Fig. 2B).

AMPK activation at low glucose is inhibited by antioxidants and independent of AMP concentration

As shown in Figs. 3A and 3B, phosphorylation of AMPK and its target ACC was significantly increased after 45 min of incubation at 1 mM glucose. The AMPK phosphorylation was rapidly reversed when glucose was added (Fig. 3D). Indeed, when 90 min at 1 mM glucose was followed by 5 min at 12 mM glucose, AMPK phosphorylation recovered its basal level. Addition of the ROS scavenger MnTBAP significantly decreased the phosphorylation of AMPK and ACC (Fig. 3B) induced by low glucose, but had no effect on AMPK activation induced by the mitochondrial uncoupler carbonyl cyanide m-chlorophenylhydrazone (CCCP) (Fig. 3C). Incubation for 10 min with 25 μM H_2O_2 also activated AMPK (Fig. 3C).

To further determine whether AMPK phosphorylation could be attributed to changes in AMP level and/or ROS production, ATP, ADP, and AMP contents were measured in cells at 1 mM glucose in the absence or presence of the antioxidant MnTBAP. ATP, ADP (data not shown), and AMP levels were not significantly altered at 1 mM glucose up to 90 min. Neither was the ATP/ADP or ATP/AMP ratio. Addition of 25 or 50 μM H_2O_2 slightly decreased AMP levels, resulting in a significant increase in the ATP/AMP ratio (Fig. 4). As expected, the mitochondrial uncoupler CCCP significantly decreased the level of ATP and increased AMP and ADP levels, resulting in a large decrease in the ATP/ADP and ATP/AMP ratios. As the activation of AMPK is elicited by very small changes in AMP concentration, assays for dose response to CCCP of ATP and AMP levels and AMPK phosphorylation were performed. Fig. 5 shows that the increase in phosphorylated AMPK occurs at measurable changes in AMP levels and ATP/AMP ratio.

Taken together, these data indicate that the superoxide produced at low glucose activates AMPK independent of changes in cellular AMP levels. However, changes in AMP level induced by mitochondrial uncoupling can induce AMPK phosphorylation independent of superoxide production.

AMPK is activated independently of LKB1 and Ca^{2+}-calmodulin-dependent kinase kinase (CaMKK)

LKB1 is an upstream kinase of AMPK that is phosphorylated at the level of two main sites, Ser307 and Ser428. Once phosphorylated, LKB1 translocates from the nucleus to the cytoplasm. We therefore explored the phosphorylation state and the intracellular localization of LKB1. Fig. 6A shows that the phosphorylation of LKB1 Ser307 was increased by exposure to low glucose concentration but not modified by addition of MnTBAP. No change in Ser428 phosphorylation was

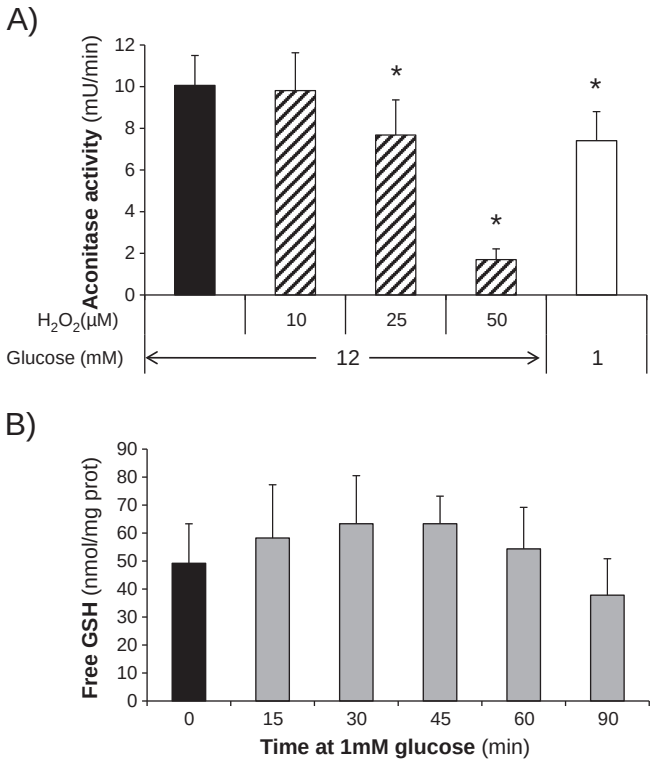

Fig. 2. Aconitase activity, but not GSH content, is decreased at low glucose. (A) Aconitase activity was measured spectrophotometrically [22] in INS1E cells after 60 min incubation at 1 mM glucose or 10 min with 10, 25, or 50 μM H_2O_2. (B) Free GSH was not altered during 1 h at 1 mM glucose, but decreased after 90 min. Means ± SEM; $n=5$; $^*p<0.05$ vs 12 mM glucose.

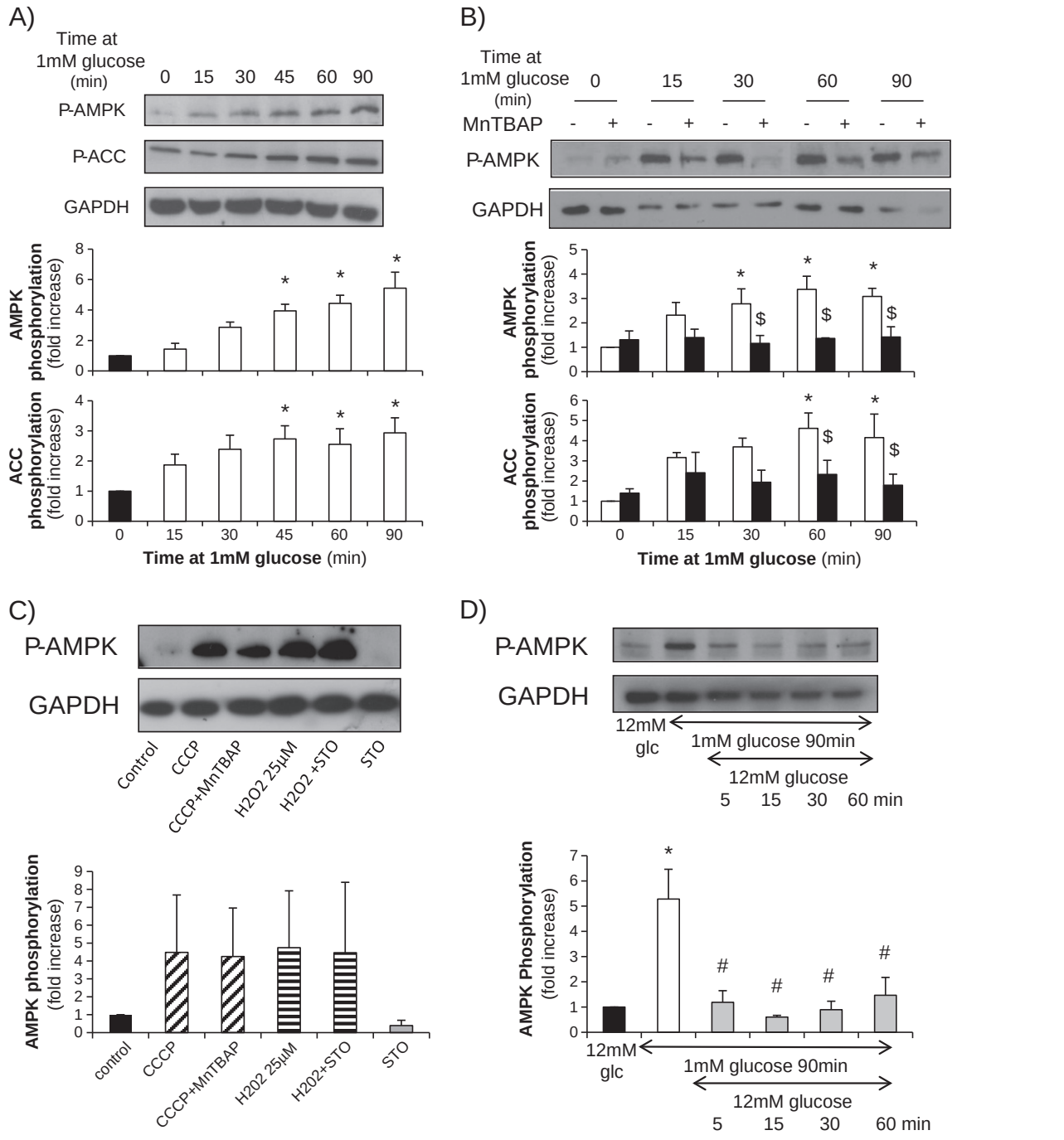

Fig. 3. Increased AMPK phosphorylation at low glucose is ROS dependent and rapidly reversible. (A) Representative experiment showing AMPK and ACC phosphorylation patterns at 1 mM glucose. Graph shows the quantification of the phosphorylation state of the two kinases, expressed in fold increase compared to time 0 ($n=4$–6). (B) Phosphorylation of AMPK and ACC was decreased by the ROS scavenger MnTBAP. White column, control; black column, MnTBAP ($n=3$–6). (C) Representative Western blot illustrating the effects of H_2O_2 and CCCP on AMPK phosphorylation. Such phosphorylation was not altered by the CaMKK inhibitor STO-609 or MnTBAP ($n=3$). (D) AMPK phosphorylation by 1 mM glucose is rapidly reversed by adding 11 mM glucose ($n=3$). Means ± SEM; $^*p<0.05$ vs time 0 (12 mM glucose), $\$p<0.05$ vs control, $\#p<0.05$ vs 90 min at 1 mM glucose.

observed at low glucose, without or with MnTBAP addition (data not shown). To confirm these data, the localization of LKB1 assessed by immunostaining was examined at high and low glucose (Fig. 6B). The LKB1 staining was located in the nucleus at 12 mM (Fig. 6B, top) and remained in the nucleus after 90 min at 1 mM glucose (Fig. 6B, bottom). Addition of antioxidant (Tempol) had no effect on LKB1 localization at low glucose concentration (Supplementary Fig. S1).

AMPK can also be phosphorylated by another upstream kinase, CaMKK. Fig. 6C shows that inhibition of CaMKK by STO-609 did not alter the phosphorylation pattern of AMPK in response to 1 mM glucose. In addition, STO-609 did not alter AMPK phosphorylation neither at 12 mM glucose nor in presence of H_2O_2 (Fig. 3C).

These data suggest that AMPK phosphorylation induced by superoxide at low glucose was independent of the LKB1 and CaMKK pathways.

Discussion

This study demonstrates that superoxide of mitochondrial origin is produced in INS1E cells at low glucose concentration and that it participates in the activation of AMPK independent of changes in

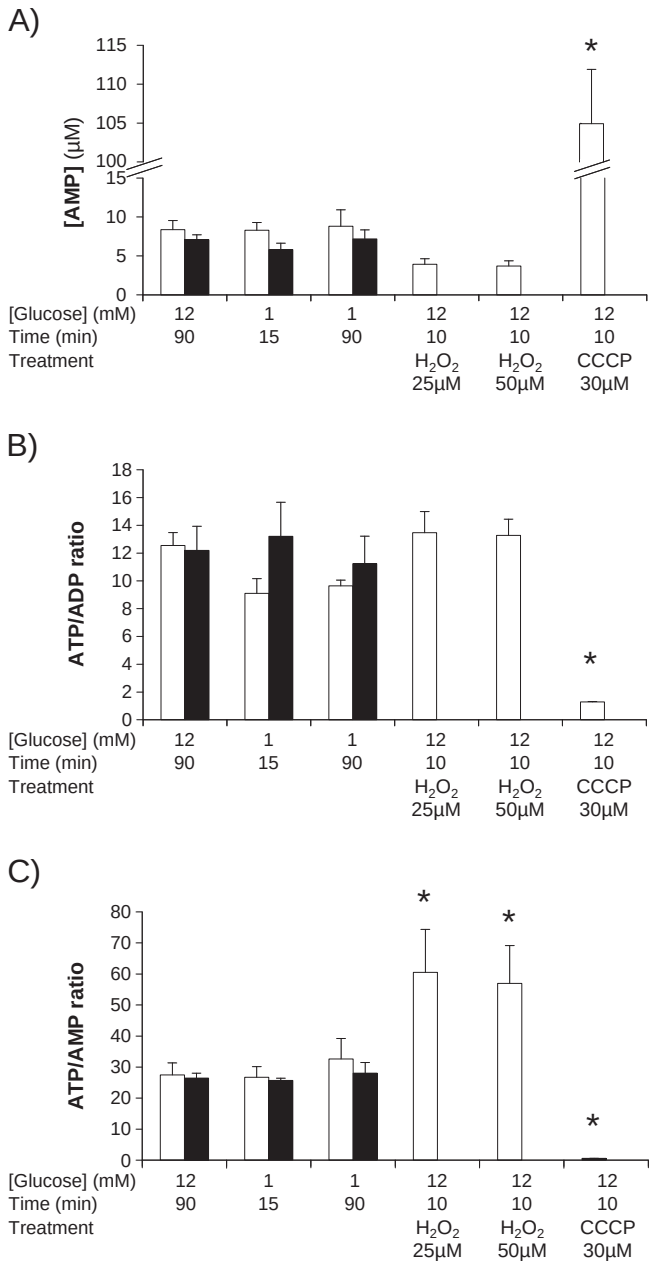

Fig. 4. AMP content and ATP/ADP and ATP/AMP ratios are not altered by treatment with 1 mM glucose. (A) AMP content of INS1E cells at 1 and 12 mM glucose under control conditions (white column) and in the presence of MnTBAP (black column). 10 min incubation in the presence of H_2O_2 had no effect, whereas the mitochondrial uncoupler CCCP significantly increased AMP content. (B) ATP/ADP ratio is altered by CCCP but 1 mM glucose and H_2O_2 had no effect. (C) ATP/AMP ratio is altered by CCCP and H_2O_2 but 90 min at 1 mM glucose had no effect ($n=3$–11). Means ± SEM; $^*p<0.05$ vs 12 mM glucose.

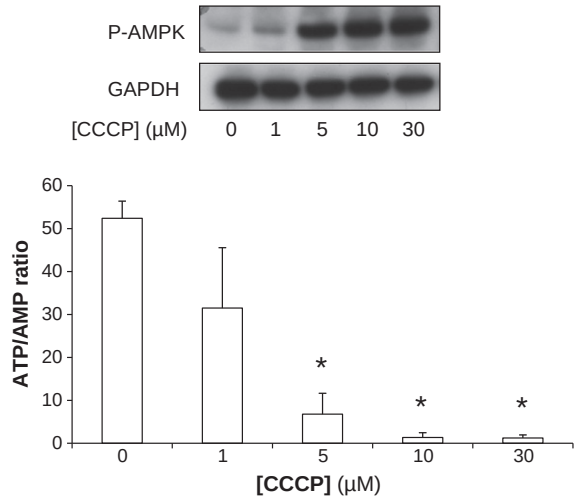

Fig. 5. Increase in AMPK phosphorylation occurs at measurable changes in ATP/AMP ratio. AMPK phosphorylation (inset) was increased when ATP/AMP ratio was significantly altered by the mitochondrial uncoupler CCCP ($n=3$; means ± SEM; $^*p<0.05$ vs control).

AMP levels. The observation that superoxide generation is increased at low glucose was initially made by Martens et al. in purified pancreatic β cells and related to decreased metabolic rate and NAD(P)H levels [15]. In insulin-secreting cell lines, long-term (12–24 h) glucose deprivation also increased ROS production [16,17]. In contrast, other studies using similar probes and/or reactive oxygen species scavengers propose that ROS are produced when glucose is increased [12,24,25] and act as signaling molecules that amplify glucose-stimulated insulin secretion [13,14]. Another recent publication using INS1E cells and a probe targeted to the mitochondria showed no significant changes in ROS production when glucose was increased from 2 to 20 mM [26]. It is difficult to explain these divergent data by technical or experimental differences between the studies. The observation by Martens et al. [15] that pancreatic β cells are heterogeneous in their metabolic response to glucose and that the high-responding cells showed a steeper decrease in ROS production after glucose addition could be an indication that the metabolic state of the cells used may be important and varies in the different studies mentioned. Furthermore, very few studies use real-time measurements of ROS generation. Based on results obtained in other cell types, it is tempting to postulate that increasing glucose will result in ROS generation. However, in pancreatic β cells, it is likely that glucose metabolism is adjusted to the capacity of the mitochondria by the amount of glucokinase, as high glucose induces ROS production only if glucokinase is overexpressed [27]. In addition, as ROS measurements are expressed in percentage or in arbitrary units, it is difficult to compare absolute levels between the different studies. In the present study, we performed real-time measurements of DHE oxidation and used attached INS1E cells and RPMI medium to minimize cellular stress. Superoxide production was linear and reaches maximum values after 60–75 min of glucose lowering. The use of inhibitors of NADPH oxidase (apocynin and DPI) or mitochondrial complex I (rotenone) or III (myxothiazol) clearly established that the ROS produced mainly originated from complex I. Superoxide production is also totally suppressed by MnTBAP, a SOD and catalase mimetic [23]. The lack of effect of NAC measured in Fig. 1C is explained by the fact that this compound is a hydrogen peroxide [28] but not a superoxide scavenger. It also provides indirect evidence that hydrogen peroxide is not measured by DHE. The increase in the rate of superoxide production during the first hour of treatment at low glucose cannot be explained by a decrease in the antioxidant system because GSH levels did not decrease during the first 90 min of low-glucose exposure. However, even if β cells are known to be antioxidant-system poor [9], and GSH represents the most important of these systems [25], fast changes in other antioxidant systems cannot be excluded. The changes in superoxide production were confirmed by measurements of aconitase activity, which showed a 25% decrease, as also measured in the presence of 25 μM H_2O_2. This enzyme is considered a mitochondrial sensor of ROS [29]. Taken together, these data suggest that INS1E cells are valuable surrogates for β cells to study the exact mechanism of ROS production at low glucose.

AMPK has been shown to be activated by an increase in AMP in response to several hormonal or metabolic stimuli such as nutrient deprivation, muscular exercise, or hypoxia. Although it is generally

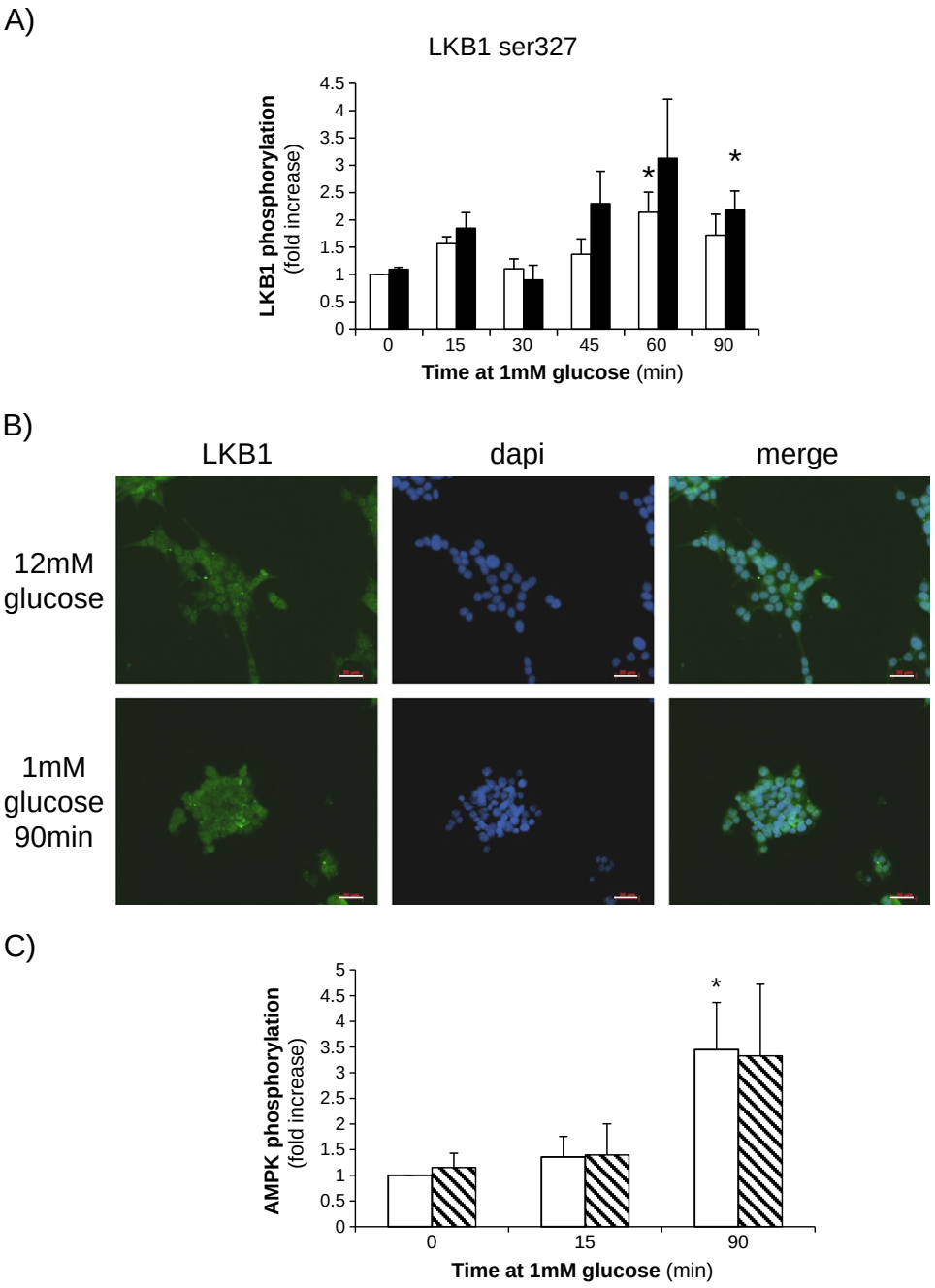

Fig. 6. AMPK phosphorylation at low glucose is independent of LKB1 and CaMKK. (A) Phosphorylation of LKB1 at Ser327 ($n=6$–9) was increased by low glucose concentration (white columns) but was not altered by the superoxide scavenger MnTBAP (black columns). (B) Representative pictures of immunohistochemistry showing that LKB1 (green) was not translocated from the nucleus (blue) to the cytosol at low glucose. Scale bar, 20 μm. (C) Inhibitor of CaMKK (STO-609; hatched column) did not alter AMPK phosphorylation at low glucose ($n=4$). Means ± SEM; $^*p<0.05$ vs time 0.

admitted that changes in AMP are the main stimulator of AMPK activity, several studies report its physiological activation by reactive oxygen or nitrogen species independent of changes in AMP levels. In mouse embryonic fibroblasts, hypoxic activation of AMPK depends on mitochondrial ROS production without changes in AMP level [30]; in the heart, ROS-induced AMPK activation participates in cardioprotection during ischemia and reperfusion injury [31]; in rat vascular smooth muscle cells, thromboxane receptor activates AMPK via hydrogen peroxide acting on LKB1, one of the AMPK upstream kinases [32]; and in prostatic carcinoma DU145 cells, ROS generated by glucose deprivation activate AMPK [33]. In the present study, AMPK activation is almost entirely prevented by MnTBAP, whereas this compound did not modify AMP levels or ATP/ADP or ATP/AMP ratio. Phosphorylated ACC followed the same pattern. The lack of change in AMP or ATP/AMP ratio after glucose deprivation may be surprising. Indeed, in HIT-15 cells, Salt et al. did not measure any change in ADP/ATP or AMP/ATP when lowering the glucose concentration to 1 mM [34]. All the changes were measured below this concentration. One could also argue that very minimal changes in AMP are required to increase AMPK activity and that our measurements are not sensitive enough. The dose response to CCCP of AMPK activation and changes in ATP/AMP ratio shows that this is not the case, as AMPK activation correlated well with the changes in adenine nucleotide ratio. For this reason, we can conclude that the changes in AMPK measured at low glucose concentration are independent of changes in AMP.

AMPK is mainly activated by two main upstream kinases, LKB1 and CaMKK [35,36]. An increase in cytosolic Ca^{2+} is unlikely to occur in β cells at low glucose concentration. Indeed, addition of STO-609, an inhibitor of CaMKK, did not modify AMPK activation at low glucose. In other studies, LKB1 was involved in ROS-induced AMPK activation without change in AMP [30]. In our study, LKB1 did not seem to be involved in such activation, because phosphorylation of Ser428 was not modified by incubation at low glucose, without or with MnTBAP (data not shown), and intracellular localization of LKB1 was not altered (Fig. 6). However, Ser327 phosphorylation was increased by low glucose without or with MnTBAP after 15 and 60 min treatment. The absence of translocation from the nucleus to the cytosol could be explained by the fact that LKB1 translocation seems to be dependent on either the phosphorylation of Ser428 [37] or the simultaneous phosphorylation of Ser428 and Ser327 [32]. Therefore, in this study, superoxide does not activate AMPK by acting on a known upstream kinase. Alternatively, it could either directly activate AMPK, by inducing oxidative modifications and *S*-glutathionylation of cystine residues of the α and β subunits of the enzyme as demonstrated in [38], or inhibit phosphatase PP2A [39,40].

The role of AMPK activation is beyond the scope of this study. Its role in glucose-stimulated insulin secretion is still a matter of debate [34,41,42]. Phosphorylation and inactivation of ACC result in a decreased level of malonyl-CoA, allowing fatty acid transport to the mitochondria and their oxidation. AMPK activation results in pancreatic β-cell death by apoptosis [43]. It also plays a role in autophagy, shown in cells in which the mTOR pathway is activated by ROS in an AMPK-dependent way [44,45]. The fact that AMPK was activated by low glucose concentration could indicate that the mTOR/autophagic pathway is activated at low glucose in a ROS- and AMPK-dependent way.

In summary, this study provides direct and indirect evidence that mitochondria-derived superoxide is produced in INS1E cells when the glucose concentration is lowered and serves as a signal for the activation of AMPK in the absence of changes in AMP. The exact mechanisms involved remain to be determined.

Acknowledgments

We thank F. Califano and Joëlle Demaison for their expert technical assistance. This study was supported by Grant 32–114134 from the Swiss National Science Foundation. The project is part of the Geneva Program for Metabolic Disorders. This article is in memory of Professor X. Leverve (1950–2010).

Appendix A. Supplementary data

Supplementary data to this article can be found online at doi:10.1016/j.freeradbiomed.2011.10.437.

References

[1] Droge, W. Free radicals in the physiological control of cell function. *Physiol. Rev.* **82:**47–95; 2002.
[2] Giacco, F.; Brownlee, M. Oxidative stress and diabetic complications. *Circ. Res.* **107:**1058–1070; 2010.
[3] Rigoulet, M.; Yoboue, E. D.; Devin, A. Mitochondrial ROS generation and its regulation: mechanisms involved in H_2O_2 signaling. *Antioxid. Redox Signal.* **14:** 459–468; 2011.
[4] Evans, J. L.; Goldfine, I. D.; Maddux, B. A.; Grodsky, G. M. Are oxidative stress-activated signaling pathways mediators of insulin resistance and beta-cell dysfunction? *Diabetes* **52:**1–8; 2003.
[5] Ristow, M.; Zarse, K.; Oberbach, A.; Kloting, N.; Birringer, M.; Kiehntopf, M.; Stumvoll, M.; Kahn, C. R.; Bluher, M. Antioxidants prevent health-promoting effects of physical exercise in humans. *Proc. Natl. Acad. Sci. U. S. A.* **106:** 8665–8670; 2009.
[6] Poitout, V.; Robertson, R. P. Glucolipotoxicity: fuel excess and beta-cell dysfunction. *Endocr. Rev.* **29:**351–366; 2008.
[7] Rabinovitch, A.; Suarez-Pinzon, W. L.; Strynadka, K.; Lakey, J. R.; Rajotte, R. V. Human pancreatic islet beta-cell destruction by cytokines involves oxygen free radicals and aldehyde production. *J. Clin. Endocrinol. Metab.* **81:**3197–3202; 1996.
[8] Grankvist, K.; Marklund, S. L.; Taljedal, I. B. CuZn-superoxide dismutase, Mn-superoxide dismutase, catalase and glutathione peroxidase in pancreatic islets and other tissues in the mouse. *Biochem. J.* **199:**393–398; 1981.
[9] Lenzen, S.; Drinkgern, J.; Tiedge, M. Low antioxidant enzyme gene expression in pancreatic islets compared with various other mouse tissues. *Free Radic. Biol. Med.* **20:**463–466; 1996.
[10] Tiedge, M.; Lortz, S.; Drinkgern, J.; Lenzen, S. Relation between antioxidant enzyme gene expression and antioxidative defense status of insulin-producing cells. *Diabetes* **46:**1733–1742; 1997.
[11] Brownlee, M. The pathobiology of diabetic complications: a unifying mechanism. *Diabetes* **54:**1615–1625; 2005.
[12] Bindokas, V. P.; Kuznetsov, A.; Sreenan, S.; Polonsky, K. S.; Roe, M. W.; Philipson, L. H. Visualizing superoxide production in normal and diabetic rat islets of Langerhans. *J. Biol. Chem.* **278:**9796–9801; 2003.
[13] Leloup, C.; Tourrel-Cuzin, C.; Magnan, C.; Karaca, M.; Castel, J.; Carneiro, L.; Colombani, A. L.; Ktorza, A.; Casteilla, L.; Penicaud, L. Mitochondrial reactive oxygen species are obligatory signals for glucose-induced insulin secretion. *Diabetes* **58:**673–681; 2009.
[14] Pi, J.; Bai, Y.; Zhang, Q.; Wong, V.; Floering, L. M.; Daniel, K.; Reece, J. M.; Deeney, J. T.; Andersen, M. E.; Corkey, B. E.; Collins, S. Reactive oxygen species as a signal in glucose-stimulated insulin secretion. *Diabetes* **56:**1783–1791; 2007.
[15] Martens, G. A.; Cai, Y.; Hinke, S.; Stange, G.; Van de Casteele, M.; Pipeleers, D. Glucose suppresses superoxide generation in metabolically responsive pancreatic beta cells. *J. Biol. Chem.* **280:**20389–20396; 2005.
[16] Cai, Y.; Martens, G. A.; Hinke, S. A.; Heimberg, H.; Pipeleers, D.; Van de Casteele, M. Increased oxygen radical formation and mitochondrial dysfunction mediate β cell apoptosis under conditions of AMP-activated protein kinase stimulation. *Free Radic. Biol. Med.* **42:**64–78; 2007.
[17] Hou, N.; Torii, S.; Saito, N.; Hosaka, M.; Takeuchi, T. Reactive oxygen species-mediated pancreatic β-cell death is regulated by interactions between stress-activated protein kinases, p38 and c-Jun N-terminal kinase, and mitogen-activated protein kinase phosphatases. *Endocrinology* **149:**1654–1665; 2008.
[18] Choi, S. L.; Kim, S. J.; Lee, K. T.; Kim, J.; Mu, J.; Birnbaum, M. J.; Soo Kim, S.; Ha, J. The regulation of AMP-activated protein kinase by H_2O_2. *Biochem. Biophys. Res. Commun.* **287:**92–97; 2001.
[19] Produit-Zengaffinen, N.; Davis-Lameloise, N.; Perreten, H.; Becard, D.; Gjinovci, A.; Keller, P. A.; Wollheim, C. B.; Herrera, P.; Muzzin, P.; Assimacopoulos-Jeannet, F. Increasing uncoupling protein-2 in pancreatic beta cells does not alter glucose-induced insulin secretion but decreases production of reactive oxygen species. *Diabetologia* **50:**84–93; 2007.
[20] Asfari, M.; Janjic, D.; Meda, P.; Li, G.; Halban, P. A.; Wollheim, C. B. Establishment of 2-mercaptoethanol-dependent differentiated insulin-secreting cell lines. *Endocrinology* **130:**167–178; 1992.
[21] Becker, L. B.; vanden Hoek, T. L.; Shao, Z. H.; Li, C. Q.; Schumacker, P. T. Generation of superoxide in cardiomyocytes during ischemia before reperfusion. *Am. J. Physiol.* **277:**H2240–H2246; 1999.
[22] Gardner, P. R. Aconitase: sensitive target and measure of superoxide. *Methods Enzymol.* **349:**9–23; 2002.
[23] Day, B. J.; Fridovich, I.; Crapo, J. D. Manganic porphyrins possess catalase activity and protect endothelial cells against hydrogen peroxide-mediated injury. *Arch. Biochem. Biophys.* **347:**256–262; 1997.
[24] Kim, W. H.; Lee, J. W.; Suh, Y. H.; Lee, H. J.; Lee, S. H.; Oh, Y. K.; Gao, B.; Jung, M. H. AICAR potentiates ROS production induced by chronic high glucose: roles of AMPK in pancreatic beta-cell apoptosis. *Cell Signal.* **19:**791–805; 2007.
[25] Tanaka, Y.; Tran, P. O.; Harmon, J.; Robertson, R. P. A role for glutathione peroxidase in protecting pancreatic beta cells against oxidative stress in a model of glucose toxicity. *Proc. Natl. Acad. Sci. U. S. A.* **99:**12363–12368; 2002.
[26] Affourtit, C.; Jastroch, M.; Brand, M. D. Uncoupling protein-2 attenuates glucose-stimulated insulin secretion in INS-1E insulinoma cells by lowering mitochondrial reactive oxygen species. *Free Radic. Biol. Med.* **50:**609–616; 2011.
[27] Wu, L.; Nicholson, W.; Knobel, S. M.; Steffner, R. J.; May, J. M.; Piston, D. W.; Powers, A. C. Oxidative stress is a mediator of glucose toxicity in insulin-secreting pancreatic islet cell lines. *J. Biol. Chem.* **279:**12126–12134; 2004.
[28] Grinberg, L.; Fibach, E.; Amer, J.; Atlas, D. N-acetylcysteine amide, a novel cell-permeating thiol, restores cellular glutathione and protects human red blood cells from oxidative stress. *Free Radic. Biol. Med.* **38:**136–145; 2005.
[29] Talbot, D. A.; Brand, M. D. Uncoupling protein 3 protects aconitase against inactivation in isolated skeletal muscle mitochondria. *Biochim. Biophys. Acta* **1709:** 150–156; 2005.
[30] Emerling, B. M.; Weinberg, F.; Snyder, C.; Burgess, Z.; Mutlu, G. M.; Viollet, B.; Budinger, G. R.; Chandel, N. S. Hypoxic activation of AMPK is dependent on mitochondrial ROS but independent of an increase in AMP/ATP ratio. *Free Radic. Biol. Med.* **46:**1386–1391; 2009.
[31] Lamberts, R. R.; Onderwater, G.; Hamdani, N.; Vreden, M. J.; Steenhuisen, J.; Eringa, E. C.; Loer, S. A.; Stienen, G. J.; Bouwman, R. A. Reactive oxygen species-induced stimulation of 5′AMP-activated protein kinase mediates sevoflurane-induced cardioprotection. *Circulation* **120:**S10–S15; 2009.
[32] Zhang, M.; Dong, Y.; Xu, J.; Xie, Z.; Wu, Y.; Song, P.; Guzman, M.; Wu, J.; Zou, M. H. Thromboxane receptor activates the AMP-activated protein kinase in vascular smooth muscle cells via hydrogen peroxide. *Circ. Res.* **102:**328–337; 2008.
[33] Yun, H.; Lee, M.; Kim, S. S.; Ha, J. Glucose deprivation increases mRNA stability of vascular endothelial growth factor through activation of AMP-activated protein kinase in DU145 prostate carcinoma. *J. Biol. Chem.* **280:**9963–9972; 2005.
[34] Salt, I. P.; Johnson, G.; Ashcroft, S. J.; Hardie, D. G. AMP-activated protein kinase is activated by low glucose in cell lines derived from pancreatic beta cells, and may regulate insulin release. *Biochem. J.* **335** (Pt 3)**:**533–539; 1998.

[35] Canto, C.; Auwerx, J. AMP-activated protein kinase and its downstream transcriptional pathways. *Cell Mol. Life Sci.* **67:**3407–3423; 2010.
[36] Witczak, C. A.; Sharoff, C. G.; Goodyear, L. J. AMP-activated protein kinase in skeletal muscle: from structure and localization to its role as a master regulator of cellular metabolism. *Cell Mol. Life Sci.* **65:**3737–3755; 2008.
[37] Xie, Z.; Dong, Y.; Scholz, R.; Neumann, D.; Zou, M. H. Phosphorylation of LKB1 at serine 428 by protein kinase C-zeta is required for metformin-enhanced activation of the AMP-activated protein kinase in endothelial cells. *Circulation* **117:** 952–962; 2008.
[38] Zmijewski, J. W.; Banerjee, S.; Bae, H.; Friggeri, A.; Lazarowski, E. R.; Abraham, E. Exposure to hydrogen peroxide induces oxidation and activation of AMP-activated protein kinase. *J. Biol. Chem.* **285:**33154–33164; 2010.
[39] Liangpunsakul, S.; Wou, S. E.; Zeng, Y.; Ross, R. A.; Jayaram, H. N.; Crabb, D. W. Effect of ethanol on hydrogen peroxide-induced AMPK phosphorylation. *Am. J. Physiol. Gastrointest. Liver Physiol.* **295:**G1173–G1181; 2008.
[40] Ravnskjaer, K.; Boergesen, M.; Dalgaard, L. T.; Mandrup, S. Glucose-induced repression of PPARalpha gene expression in pancreatic beta-cells involves PP2A activation and AMPK inactivation. *J. Mol. Endocrinol.* **36:**289–299; 2006.
[41] Dufer, M.; Noack, K.; Krippeit-Drews, P.; Drews, G. Activation of the AMP-activated protein kinase enhances glucose-stimulated insulin secretion in mouse beta-cells. *Islets* **2:**156–163; 2010.
[42] Gleason, C. E.; Lu, D.; Witters, L. A.; Newgard, C. B.; Birnbaum, M. J. The role of AMPK and mTOR in nutrient sensing in pancreatic beta-cells. *J. Biol. Chem.* **282:** 10341–10351; 2007.
[43] Cai, Y.; Wang, Q.; Ling, Z.; Pipeleers, D.; McDermott, P.; Pende, M.; Heimberg, H.; Van de Casteele, M. Akt activation protects pancreatic beta cells from AMPK-mediated death through stimulation of mTOR. *Biochem. Pharmacol.* **75:**1981–1993; 2008.
[44] Chen, L.; Xu, B.; Liu, L.; Luo, Y.; Yin, J.; Zhou, H.; Chen, W.; Shen, T.; Han, X.; Huang, S. Hydrogen peroxide inhibits mTOR signaling by activation of AMPKalpha leading to apoptosis of neuronal cells. *Lab. Invest.* **90:**762–773; 2010.
[45] Li, M.; Zhao, L.; Liu, J.; Liu, A.; Jia, C.; Ma, D.; Jiang, Y.; Bai, X. Multi-mechanisms are involved in reactive oxygen species regulation of mTORC1 signaling. *Cell Signal.* **22:**1469–1476; 2010.